Surface Science 653 (2016) 138–142

Contents lists available at ScienceDirect

Surface Science

journal homepage: www.elsevier.com/locate/susc

Adsorption and self-assembly of fullerenes on Si(111)$\sqrt{3} \times \sqrt{3}$-Ag: C_{60} versus C_{70}

D.A. Olyanich[a,b], V.V. Mararov[a,b], T.V. Utas[a,b], A.V. Zotov[a,b,c,*], A.A. Saranin[a,b]

[a] Institute of Automation and Control Processes FEB RAS, 690041 Vladivostok, Russia
[b] School of Natural Sciences, Far Eastern Federal University, 690950 Vladivostok, Russia
[c] Department of Electronics, Vladivostok State University of Economics and Service, 690600 Vladivostok, Russia

ARTICLE INFO

Article history:
Received 30 April 2016
Received in revised form 27 June 2016
Accepted 28 June 2016
Available online 4 July 2016

Keywords:
Molecular–solid interactions
Silicon
Fullerene
Self–assembly
Adsorption
Scanning tunneling microscopy

ABSTRACT

Behavior of C_{60} and C_{70} fullerenes adsorbed onto Si(111)$\sqrt{3} \times \sqrt{3}$-Ag is compared on the basis of STM observations. Such characteristics as sticking coefficient, migration rate, attachment/detachment rate from the molecular islands are considered. Room-temperature sticking coefficient for C_{70} is slightly greater than that for C_{60}. Due to their non-spherical shape, C_{70} are less mobile than spherical C_{60}. For both types of fullerenes, mobility of molecules on the fullerene layer is significantly retarded as compared to that on bare Si(111)$\sqrt{3} \times \sqrt{3}$-Ag surface. Self-assembly of C_{60} obeys layer-by-layer growth mode, while C_{70} follows multi-layer mode, a sign of a greater Ehrlich-Schwoebel barrier. Alternating deposition of C_{60} and C_{70} paves the way to fabricate planar C_{60}/C_{70} heterostructures with the most promising results being obtained with nanostructured islands grown on C_{60} monomolecular layer.

© 2016 Elsevier B.V. All rights reserved.

1. Introduction

Fullerene adsorption and self-assembly on the various metal and semiconductor surfaces attract considerable interest, in particular, due to potentially valuable applications of fullerene layers in nanoscale devices. Metal-induced reconstructions on semiconductor (e.g., Si) surfaces show up as a specific class of template surfaces, that differ essentially in structure and properties from both pure metal and semiconductor surfaces. If one addresses C_{60} interaction with various metal-reconstructed Si surfaces, the Si(111)$\sqrt{3} \times \sqrt{3}$-Ag surface opens the list of the most extensively studied templates [1–9]. The high-quality homogeneous Si(111)$\sqrt{3} \times \sqrt{3}$-Ag surface with a negligible density of point defects can be easily prepared just by saturating adsorption of Ag on the Si(111)7 × 7 surface held at about 500 °C. Atomic arrangement of the Si(111)$\sqrt{3} \times \sqrt{3}$-Ag surface is well-established to be described by the inequivalent triangle (IET) model [10, 11]. Thus, bearing in mind the available background, easy preparation of high-quality surface and well-established atomic structure, the Si(111)$\sqrt{3} \times \sqrt{3}$-Ag reconstruction is believed to be an appropriate playground for studying fine effects of fullerene adsorption, in particular the role of fullerene size and shape.

In the present paper, we report on the results of comparative study of C_{60} and C_{70} adsorption and self-assembly on Si(111)$\sqrt{3} \times \sqrt{3}$-Ag surface. Using scanning tunneling microscopy (STM) observations at room temperature (RT) and 115 K, we have addressed such characteristics as sticking coefficient, migration rate, attachment/detachment rate from the molecular islands for C_{60} and C_{70} fullerenes. Estimations for some of these parameters have been acquired. In conclusion, we have considered possibility of growing planar C_{60}/C_{70} heterostructures using alternating deposition of C_{60} and C_{70} and demonstrated that the most vivid results can be obtained with fullerene nanostructured islands grown on fullerene monomolecular layer.

2. Experiment

Our experiments were performed with an Omicron VT-STM operating in an ultrahigh vacuum (~2.0×10^{-10} Torr). Atomically-clean Si(111)7 × 7 surfaces were prepared in situ by flashing to 1280 °C after the samples were first outgassed at 600 °C for several hours. Silver was deposited from an Ag-wrapped tungsten filament. The

* Corresponding author.
E-mail address: zotov@iacp.dvo.ru (A. Zotov).

http://dx.doi.org/10.1016/j.susc.2016.06.016
0039-6028/© 2016 Elsevier B.V. All rights reserved.

high-quality Si(111)$\sqrt{3} \times \sqrt{3}$-Ag surface with a negligible density of point defects was prepared by saturating adsorption of about 1 ML Ag onto the Si(111)7 × 7 surface held at 500 °C. Fullerenes, C_{60} (Alfa Aesar, purity 99.92%) and C_{70} (BuckyUSA, purity 99.5%), were deposited from resistively heated Ta boats. For STM observations, electrochemically etched tungsten tips cleaned by *in situ* heating were employed.

3. Results and discussion

In agreement with the previous STM studies, we have found that upon RT adsorption onto Si(111)$\sqrt{3} \times \sqrt{3}$-Ag surface C_{60} fullerenes self-assemble into the close-packed hexagonal arrays in two azimuthal orientations, i.e. with C_{60} molecular rows making an angle of either 19.1° (19.1°-rotated arrays) or 30° (30°-rotated arrays) with the main crystallographic direction of Si(111), [$\bar{1}$10]. The 19.1°-rotated arrays definitely prevail over 30°-rotated arrays (Fig. 1a). Other orientations of the C_{60} arrays can also occur occasionally. For example, presence of the Si(111)6 × 1-Ag domains on the surface can trigger the growth of 0°-rotated arrays (i.e., those where C_{60} rows are aligned along the [$\bar{1}$10] direction). In order to avoid this effect, we have ensured that the $\sqrt{3} \times \sqrt{3}$-Ag reconstruction occupies the entire surface in all experiments. Like C_{60} molecules, C_{70} fullerenes also self-assemble into the close packed hexagonal arrays, but with the different orientations. For C_{70}, the 0°-rotation is the major orientation followed by the 30°-rotation (Fig. 1b).

Peculiar feature of the C_{60} monolayers is a presence of the dark features within fullerene arrays [3, 8]. They were first interpreted as missing-molecule defects [3], but have recently been recognized as "dim C_{60}" fullerenes residing ~1.6 Å lower than the other ("normal") C_{60} fullerenes due to disintegration of Ag trimers on Si(111)$\sqrt{3} \times \sqrt{3}$-Ag under given fullerenes [8]. While the normal C_{60} are in continuous rotation, the dim C_{60} are fixed in one of the single orientations, indicating a tight binding to the surface [8]. C_{70} arrays also contain dim fullerenes which have the same origin, namely they are located lower than other molecules and are fixed in certain orientations (Fig. 2a). As a result, they display characteristic intermolecular structures in the high-resolution filled-state STM images (Fig. 2b, c, d, e, f). It is worth noting that behavior of dim C_{70} fullerenes appears very similar to that of dim C_{60} [8]. An additional feature which is specific for C_{70} arrays is that the "normal" fullerenes display somewhat different STM contrast. This is clearly seen in Fig. 2a where neighboring C_{60} and C_{70} arrays are shown. The difference can reasonably be attributed to variety of adsorption geometries for the non-spherical C_{70} molecules (e.g., with "standing", "lying" and "inclined" molecules). The vertically standing C_{70} fullerenes display the brightest STM contrast and they can be considered as superbright C_{70}. The other specific feature is a presence of vacancies (i.e., real missing-molecule defects) within C_{70} arrays, but their occurrence is actually very seldom. They are shown in Fig. 2g and h, including the vacancy which became filled by C_{70} in the course of STM scanning (Fig. 2h).

When the deposited fullerene coverage is close to one monomolecular layer, essential difference in the fullerene layer morphology becomes apparent for C_{60} and C_{70} (Fig. 3). The C_{60} growth follows almost ideal layer-by-layer mode, namely, patches of the second molecular layer appear only when the first layer is close to completion (Fig. 3a). In contrast, the growth mode for C_{70} is almost multi-layer one, in which case growth of the second and even the third layers start well before completion of the first layer (Fig. 3b). The change of the growth mode from layer-by-layer to multi-layer one might be caused either by suppressed fullerene migration over the first molecular layer or by the presence of the noticeable Ehrlich-Schwoebel barrier that hampers crossing molecular step by the

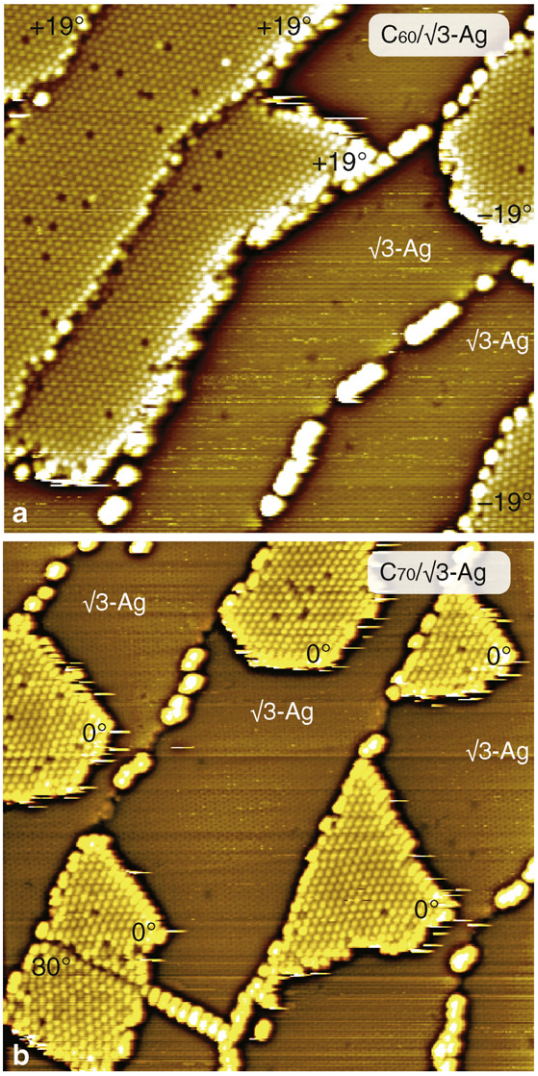

Fig. 1. 750×750 Å^2 STM images of (a) C_{60} and (b) C_{70} arrays grown on Si(111)$\sqrt{3}\times\sqrt{3}$-Ag surface at RT. The orientations of the arrays (i.e., angles which molecular rows make with the main crystallographic direction of Si(111), [$\bar{1}$10]) are indicated.

fullerenes (i.e., fullerene jumping down to the $\sqrt{3} \times \sqrt{3}$-Ag surface). To elucidate, at least semi-quantitatively, these characteristics as well as some others, we have explored fullerene behavior not only at RT, but also at low temperature of ~115 K.

In particular, it was noticed that after similar doses, fullerene coverages at RT were systematically lower than those at 115 K, that means that fullerene sticking probability s is not equal 1.0 at RT. Assuming $s = 1.0$ for adsorption at 110 K, it was found that s is about 0.6–0.7 for RT C_{60} adsorption onto Si(111)$\sqrt{3} \times \sqrt{3}$-Ag and ~0.8 for C_{70} under the same conditions. Remarkably, heating of the molecular layers formed at 115 K to RT does not change the fullerene coverage. Thus, one can conclude that there are plausibly two adsorption states of fullerene at Si(111)$\sqrt{3}\times\sqrt{3}$-Ag. The first one is the precursor state when fullerene migrates over the terrace and might desorb from the surface. The second one is the stable state when fullerene becomes attached to atomic step or fullerene array.

Let us characterize now surface migration of fullerenes in the framework of the rate equation theory which establishes a quantitative relation between island density N as a function of deposition rate R and growth temperature T and characteristics of the processes

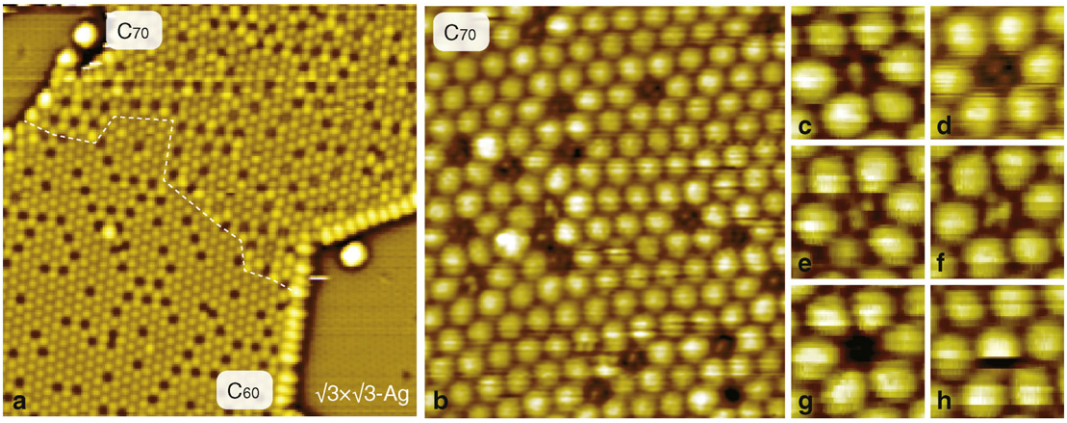

Fig. 2. (a) 380 × 380 Å^2 STM image of coexisted C_{60} and C_{70} arrays with a boundary between them indicated by a dashed white line. (b) Enlarged (110 × 130 Å^2) filled-state STM image of the C_{70} array. (c, d, e, f) Typical intermolecular structures of dim C_{70}. (g) Missing-molecular defect and (h) missing-molecular defect dynamically filled by C_{70} molecule.

involved in island formation, including a surface diffusion barrier, a critical island size i and a binding energy gained in forming a critical island [12]. However, accurate determination of all these characteristics requires comprehensive measurements in the wide ranges of temperature and deposition rate. In the present study, we have limited our consideration by a semi-quantitative comparison for different fullerenes, C_{60} and C_{70}, and different surfaces, Si(111)$\sqrt{3} \times \sqrt{3}$-Ag and fullerene monolayer at fixed temperature and deposition rate. Rate equation theory yields a relation of the type, $N \propto \left(\frac{R}{D}\right)^{i/(i+2)}$ [12], where D is the diffusion coefficient. Assuming $i = 1$ (that seems a reasonable guess which holds for a number of fullerene/substrate systems [13–15]), one obtains a relation, $D \propto N^{-3}$.

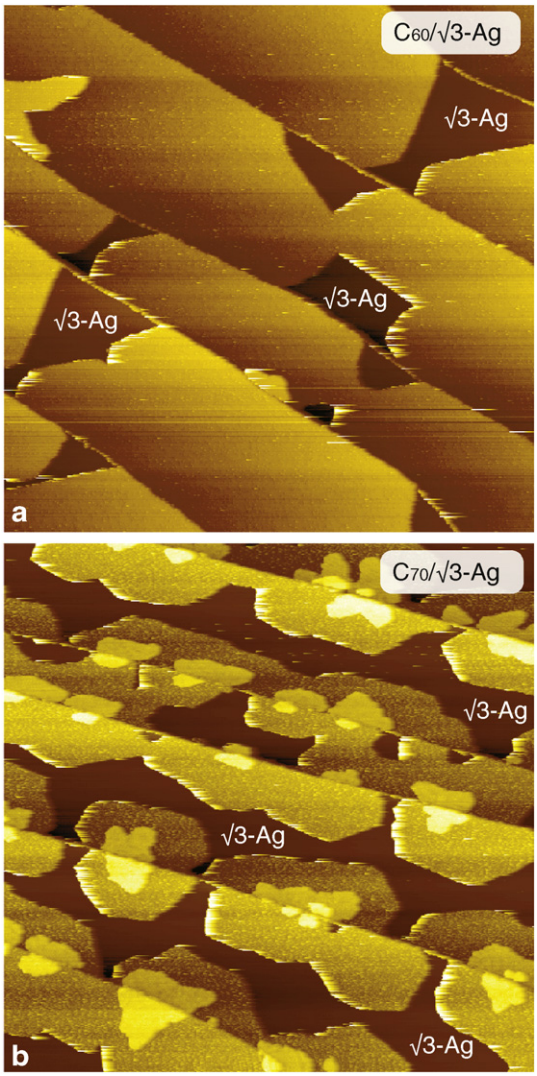

Fig. 3. 4000 × 4000 Å^2 STM images of (a) C_{60} and (b) C_{70} layers after depositing about 0.8 monomolecular layer of fullerenes onto Si(111)$\sqrt{3} \times \sqrt{3}$-Ag surface held at RT.

STM observations have revealed that both C_{60} and C_{70} fullerenes are highly mobile on Si(111)$\sqrt{3} \times \sqrt{3}$-Ag surface even at $T = 115$ K and most of the fullerenes reach the atomic steps to form islands there (see Fig. 4a, showing C_{70} islands, as an example). Individual islands are seldom and they can be found only at relatively wide terraces. As a result, statistics for evaluation of island density is relatively poor, hence the obtained values can be considered only as rough estimations. We obtained an island density of ~0.8×10^{-4} nm^{-2} and ~2.0×10^{-4} nm^{-2} for C_{60} and C_{70}, respectively, on Si(111)$\sqrt{3} \times \sqrt{3}$-Ag at 115 K. Thus, C_{60} migrate faster than C_{70} with the ratio of diffusion coefficients being ~16. This difference can be visualized also as lowering the diffusion barrier by ~27 meV. The lower rate of C_{70} surface diffusion can be attributed to their non-spherical shape bearing in mind that rolling is rather typical for fullerene motion on surfaces.

Mobility of fullerenes on top of the monomolecular layer is strongly retarded compared to that on the Si(111)$\sqrt{3} \times \sqrt{3}$-Ag surface. This effect is evidenced by the considerable increase of fullerene island density (Fig. 4b). The island density of C_{60} on C_{60} layer at 115 K is ~2.0×10^{-3} nm^{-2} and that of C_{70} on C_{70} layer is ~3.3×10^{-3} nm^{-2}. Evaluation shows that changing Si(111)$\sqrt{3} \times \sqrt{3}$-Ag surface for fullerene layer increases diffusion barrier by ~80–90 meV for both C_{60} and C_{70}. This is a natural sequence of the fact that the binding between fullerenes is greater than binding of fullerene with Si(111)$\sqrt{3} \times \sqrt{3}$-Ag surface. If compare the diffusion barriers for C_{60} on C_{60} layer and C_{70} on C_{70} layer, the latter is higher by ~15 meV. One can see that the difference is minor. Therefore, returning to the difference in the fullerene growth mode, layer-by-layer for C_{60} and multi-layer for C_{70}, one has to admit that the possible difference in the Ehrlich-Schwoebel barrier might play there a decisive role.

Having two types of fullerenes, C_{60} and C_{70}, we have examined possibility of growing planar heterostructures composed of fullerenes of both types when C_{60} deposition is alternated by C_{70} deposition and vice versa. As an example, Fig. 5 shows a result of successive deposition of C_{60} and C_{70}. For better visualization,

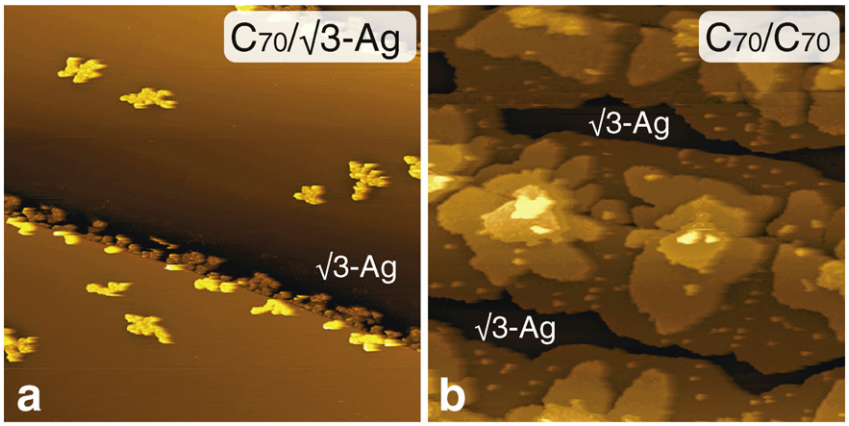

Fig. 4. 4000 × 4000 Å^2 STM images illustrating low-temperature (T = 115 K) C_{70} fullerene island growth on (a) Si(111)$\sqrt{3} \times \sqrt{3}$-Ag surface and (b) C_{70} layers.

preparation of the particular sample included C_{60} deposition at 115 K, followed by heating sample to RT and subsequent C_{70} deposition conducted also at RT. The observations have allowed us to derive several conclusions. In particular, it has been found that the already formed fullerene arrays can produce an alignment effect on the fullerene arrays grown at the next step. For example, C_{60} arrays on Si(111)$\sqrt{3} \times \sqrt{3}$-Ag surface can induce formation of C_{70} arrays with non-typical 19.1°-rotated orientation. One can also notice that a sharp boundary between C_{60} and C_{70} arrays on Si(111)$\sqrt{3} \times \sqrt{3}$-Ag surface is lacking and there is a region where C_{60} and C_{70} fullerenes are intermixed. [Remind that all "normal" C_{60} fullerenes display the same STM contrast, while for C_{70} it is variable.] We speculate that fullerene intermixing could hardly be caused by interdiffusion of fullerenes within a close-packed molecular layer, since it could efficiently occur only in the presence of sufficient density of molecular vacancies which are actually lacking in STM images. A more realistic guess is associated with the fact that at RT fullerene islands are in a dynamical equilibrium with fullerene two-dimensional molecular gas present on Si(111)$\sqrt{3} \times \sqrt{3}$-Ag surface. As a result, the shape and size of fullerene islands change continuously due attachment (detachment) of fullerenes to (from) the island edge. Thus, C_{60} and C_{70} can intermix already in the two-dimensional molecular gas phase.

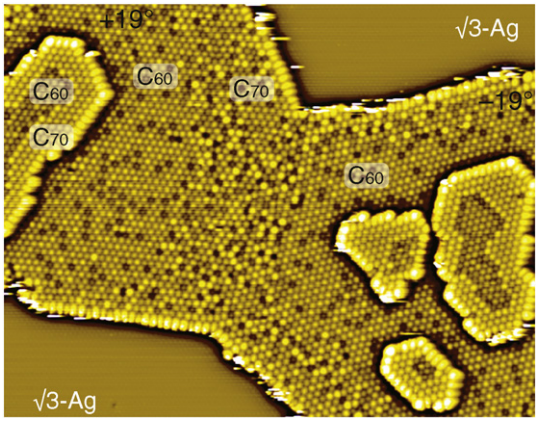

Fig. 5. 750 × 600 Å^2 STM image of the fullerene arrays formed by successive deposition of C_{60} and C_{70} onto Si(111)$\sqrt{3} \times \sqrt{3}$-Ag surface held at RT. The STM image was high-pass-filtered.

Formation of the planar fullerene heterostructures becomes more feasible when the islands are grown on the fullerene monomolecular layer. Fig. 6 shows the example nanostructured islands obtained by alternating deposition of C_{60} and C_{70} after various numbers of deposition steps. In this experiment, we used C_{60} monolayer as a template and initial inoculating islands were also built of C_{60} molecules. One can see a definite contrast difference between fullerenes of two types: C_{70} look brighter than C_{60}. Remarkably, that all C_{70} residing on C_{60} layer demonstrate the same brightness that is in contrast to C_{70} on Si(111)$\sqrt{3} \times \sqrt{3}$-Ag surface (Fig. 5). Brightness similarity of C_{70} forming array on the C_{60} layer plausibly means that all C_{70} stand vertically to adopt an epitaxial relationship with underlying C_{60} template. One can see also that boundaries between C_{60} and C_{70} arrays are rather sharp. The possible reason why the boundaries within the islands grown on fullerene monolayer are sharper than those in the islands grown on Si(111)$\sqrt{3} \times \sqrt{3}$-Ag surface is associated with the greater coordination number of fullerenes at the island edge in the former case leading to suppressed detachment rate of those fullerenes. However, it is not suppressed completely, hence boundaries are still not ideal.

4. Conclusions

In conclusion, adsorption and layer growth of C_{60} and C_{70} on Si(111)$\sqrt{3} \times \sqrt{3}$-Ag has been studied using STM observations and a certain difference in their behavior was detected. In particular, it has been found that room-temperature sticking coefficient of C_{60} is lower (0.65 versus 0.8) and C_{60} are more mobile as compared to C_{70} that can be visualized by lowering the diffusion barrier by ~27 meV. For both types of fullerenes, mobility of molecules on the fullerene layer is significantly retarded as compared to that on bare Si(111)$\sqrt{3} \times \sqrt{3}$-Ag surface with increase of the diffusion barrier by ~80–90 meV. While C_{60} obey layer-by-layer growth mode, C_{70} follow multi-layer mode, a sign of a greater Ehrlich-Schwoebel barrier. Alternating deposition of C_{60} and C_{70} has been shown to pave the way to fabricate planar C_{60}/C_{70} heterostructures with the most promising results being obtained with fullerene islands grown on C_{60} monolayer.

Acknowledgments

The work was supported by Russian Science Foundation under Grant No. 14-12-00482.

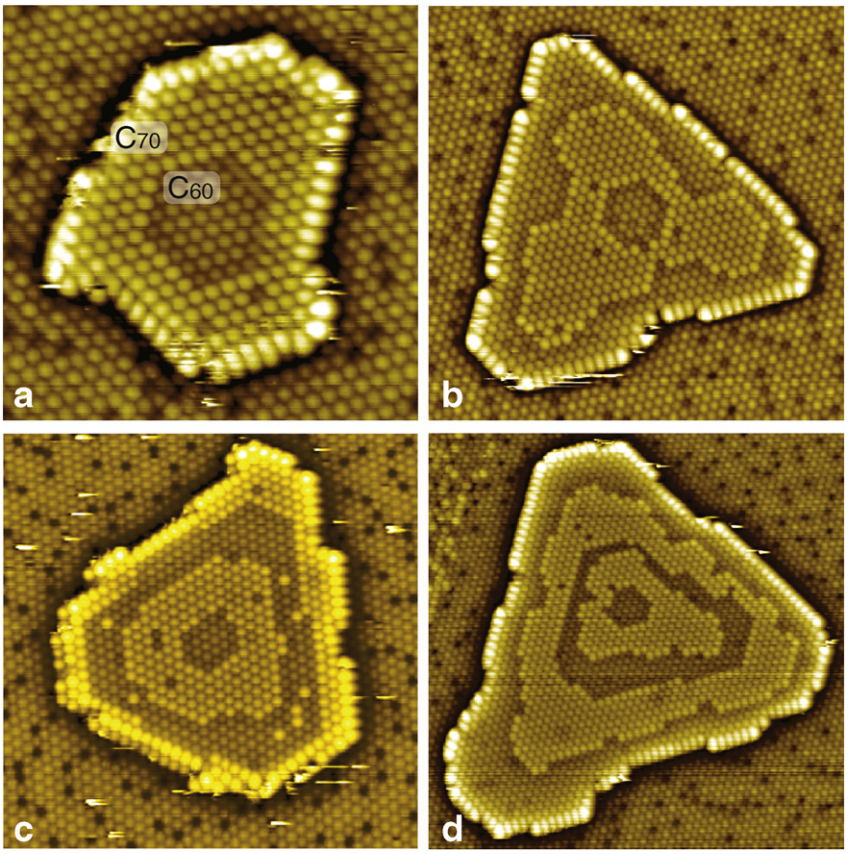

Fig. 6. Examples of nanostructured fullerene islands on C_{60} monolayer fabricated by alternating deposition of C_{60} and C_{70} at RT using (a) two-step, (b) three-step, (c) four-step and (d) five-step deposition cycles. All STM images were high-pass-filtered.

References

[1] M.D. Upward, P. Moriarty, P.H. Beton, Double domain ordering and selective removal of $_{C60}$ on Ag/Si(111)-($\sqrt{3} \times \sqrt{3}$)$R30^\circ$, Phys. Rev B 56 (1997) R1704.

[2] G.L. LeLay, M. Göthelid, V.Y. Aristov, A. Cricenti, M.C. Håkansson, C. Giammichele, P. Perfetti, J. Avila, M.C. Asensio, Adsorption of C_{60} on Si(111)$\sqrt{3} \times \sqrt{3}$R(30°)-Ag, Surf. Sci. (1997) 377–379, 1061.

[3] T. Nakayama, J. Onoe, K. Takeuchi, M. Aono, Weakly bound and strained C_{60} monolayer on the Si(111)$\sqrt{3} \times \sqrt{3}R30^\circ$-Ag substrate surface, Phys. Rev B 59 (1999) 12627.

[4] K. Tsuchie, T. Nagao, S. Hasegawa, Structure of C_{60} layers on the Si(111)-$\sqrt{3} \times \sqrt{3}$-Ag surface, Phys. Rev. B 60 (1999) 11131.

[5] S. Hasegawa, K. Tsuchie, K. Toriyma, X. Tong, T. Nagao, Surface electronic transport on silicon: donor- and acceptor-type adsorbates on Si(111)-$\sqrt{3} \times \sqrt{3}$-Ag substrate, Appl. Surf. Sci. (2000) 162–163, 42.

[6] M. Nakaya, T. Nakayama, Y. Kuwahara, M. Aono, Fabrication of nanostructures by selective growth of C_{60} and Si on Si(111) substrate, Surf. Sci. 600 (2006) 2810.

[7] S. Jeong, Atomic and electronic structures of a fullerene molecule on a Ag/Si(111)$\sqrt{3} \times \sqrt{3}$surface, J. Phys. Soc. Jap. 79 (2010) 074603.

[8] D.V. Gruznev, A.V. Matetskiy, L.V. Bondarenko, A.V. Zotov, A.A. Saranin, J.P. Chou, C.M. Wei, Y.L. Wang, Dim C_{60} fullerenes on Si(111)$\sqrt{3} \times \sqrt{3}$-Ag surface, Surf. Sci. 612 (2013) 31.

[9] D.A. Tsukanov, M.V. Ryzhkova, E.A. Borisenko, L.V. Bondarenko, A.V. Matetskiy, D.V. Gruznev, A.V. Zotov, A.A. Saranin, Effect of C_{60} layer on the growth mode and conductance of Au and Ag films on Si(111)$\sqrt{3}$-Au and Si(111)$\sqrt{3}$-Ag surfaces, J. Appl. Phys. 110 (2011)093704.

[10] H. Aizawa, M. Tsukada, N. Sato, S. Hasegawa, Asymmetric structure of the Si(111)-$\sqrt{3} \times \sqrt{3}$-Ag surface, Surf. Sci. 429 (1999) L509.

[11] N. Sato, T. Nagao, S. Hasegawa, Si(111)-($\sqrt{3} \times \sqrt{3}$)-Ag surface at low temperatures: symmetry breaking and surface twin boundaries, Surf. Sci. 442 (1999) 65.

[12] J.A. Venables, G.D.T. Spiller, M. Hanbücken, Nucleation and growth of thin films, Rep. Prog. Phys. 47 (1984) 399.

[13] F. Loske, J. Lübbe, J. Schütte, M. Reichling, A. Kühnle, Quantitative description of C_{60} diffusion on an insulating surface, Phys. Rev. B 82 (2010)155428.

[14] A.V. Matetskiy, L.V. Bondarenko, D.V. Gruznev, A.V. Zotov, A.A. Saranin, J.P. Chou, C.R. Hsing, C.M. Wei, Y.L. Wang, Peculiar diffusion of C_{60} on In-adsorbed Si(111)$\sqrt{3} \times \sqrt{3}$-Au surface, Surf. Sci. 616 (2013) 44.

[15] N.V. Sibirev, V.G. Dubrovskii, A.V. Matetskiy, L.V. Bondarenko, D.V. Gruznev, A.V. Zotov, A.A. Saranin, Size distribution of fullerene surface clusters, Appl. Surf. Sci. 307 (2014) 46.